Biochemical and Biophysical Research Communications 443 (2014) 950–956

Contents lists available at ScienceDirect

Biochemical and Biophysical Research Communications

journal homepage: www.elsevier.com/locate/ybbrc

Neovessel formation promotes liver fibrosis via providing latent transforming growth factor-β

Kotaro Sakata [a,b,c], Satoshi Eda [a], Eun-Seo Lee [a], Mitsuko Hara [a], Masaya Imoto [b], Soichi Kojima [a,*]

[a] Micro-signaling Regulation Technology Unit, RIKEN Center for Life Science Technologies, Wako, Saitama 351-0198, Japan
[b] Department of Biosciences and Informatics, Faculty of Science and Technology, Keio University, Yokohama, Kanagawa 223-8522, Japan
[c] Drug Discovery Laboratory, Wakunaga Pharmaceutical Co., Ltd., Akitakata, Hiroshima 739-1195, Japan

ARTICLE INFO

Article history:
Received 10 December 2013
Available online 19 December 2013

Keywords:
Transforming growth factor-β
Liver fibrosis
Hepatic stellate cells
Liver sinusoidal endothelial cells

ABSTRACT

Aim: Hepatic fibrosis and angiogenesis occur in parallel during the progression of liver disease. Fibrosis promotes angiogenesis via inducing vascular endothelial growth factor (VEGF) from the activated hepatic stellate cells (HSCs). In turn, increased neovessel formation causes fibrosis, although the underlying molecular mechanism remains undetermined. In the current study, we aimed to address a role of endothelial cells (ECs) as a source of latent transforming growth factor (TGF)-β, the precursor of the most fibrogenic cytokine TGF-β.
Methods: After recombinant VEGF was administered to mice via the tail vein, hepatic angiogenesis and fibrogenesis were evaluated using immunohistochemical and biochemical analyses in addition to investigation of TGF-β activation using primary cultured HSCs and liver sinusoidal ECs (LSECs).
Results: In addition to increased hepatic levels of CD31 expression, VEGF-treated mice showed increased α-smooth muscle actin (α-SMA) expression, hepatic contents of hydroxyproline, and latency associated protein degradation products, which reflects cell surface activation of TGF-β via plasma kallikrein (PLK). Liberating the PLK-urokinase plasminogen activator receptor complex from the HSC surface by cleaving a tethering phosphatidylinositol linker with its specific phospholipase C inhibited the activating latent TGF-β present in LSEC conditioned medium and subsequent HSC activation.
Conclusion: Neovessel formation (angiogenesis) accelerates liver fibrosis at least in part via provision of latent TGF-β that activated on the surface of HSCs by PLK, thereby resultant active TGF-β stimulates the activation of HSCs.

1. Introduction

Liver fibrosis, a common feature of almost all chronic liver diseases, is caused by the excessive accumulation of extracellular matrix (ECM) proteins, including collagen produced mainly by hepatic stellate cells (HSCs) through the process termed activation [1–3]. Under physiological conditions, quiescent HSCs embrace sinusoids as liver-specific pericytes. When the liver parenchyma is chronically injured by various causes, HSCs detach from the sinusoids and subsequently transform into myofibroblast-like cells. This HSC activation is characterized by a loss of lipid droplets, the enhanced production of ECM, and the expression of activation markers such as α-smooth muscle actin (α-SMA) [4]. The HSC activation process is regulated by both autocrine and paracrine growth factors [4,5], among which transforming growth factor (TGF)-β, the most fibrogenic cytokine, plays a critical role [6,7].

TGF-β is produced as a high molecular weight latent form with its propeptide region known as "latency associated protein (LAP)", and thereby must be activated before exerting its biological activity [8]. Latent TGF-β is activated by plasma kallikrein (PLK), which is bound to glycophosphatidylinositol-anchored urokinase-type plasminogen activator receptor (uPAR) on the cell surface and released by phosphatidylinositol-specific phospholipase C (PI-PLC) [9]. PLK cleaves LAP between R58 and L59 during liver fibrosis [10]. After cleavage, the N-terminal side LAP degradation products ending at R58 (R58 LAP-DPs) remain within the ECM of the liver tissues through LTBP, serving as a footprint for active TGF-β generation. We produced a specific antibody (anti-R58 antibody) that detects a neoepitope at the cutting edge of R58 LAP-DPs [10].

Angiogenesis in the adult liver occurs both in pathological settings, such as cirrhosis and tumor development, and in physiological conditions such as liver regeneration [11,12]. Blood vessels in the liver are classified into the hepatic artery, portal vein and sinusoidal blood vessel groups. Thus, liver sinusoidal endothelial

* Corresponding author. Address: Micro-signaling Regulation Technology Unit, RIKEN Center for Life Science Technologies, 2-1 Hirosawa, Wako, Saitama 351-0198, Japan. Fax: +81 48 462 4675.
E-mail address: skojima@riken.jp (S. Kojima).

0006-291X/$ - see front matter © 2013 Elsevier Inc. All rights reserved.
http://dx.doi.org/10.1016/j.bbrc.2013.12.074

cells (LSECs) are the largest population of endothelial cells in the liver.

Hepatic angiogenesis and fibrogenesis occur in parallel during liver diseases [11,13]. Sahin et al. showed that VEGF transgenic mice with increased serum VEGF concentrations have augmented liver fibrosis [14]. However, how the overproduction of VEGF induces liver fibrosis has not yet been determined.

The current study addressed a role of ECs as a source of latent TGF-β, the precursor of the most fibrogenic cytokine TGF-β.

2. Materials and methods

2.1. Materials

Fluorescein isothiocyanate (FITC)-conjugated rat anti-mouse CD31 monoclonal antibody (Clone 390) and rat anti-mouse CD146 monoclonal antibody (Clone ME-9F1) were purchased from Millipore (Billerica, MA, USA) and Bio Legend (San Diego, CA, USA), respectively. FITC-conjugated mouse anti-α-SMA monoclonal antibody (Clone 1A4) and anti-α-SMA monoclonal antibody (Clone 1A4) were purchased from Sigma–Aldrich (St. Louis, MO, USA) and Dako (Glostrup, Denmark), respectively. Neutralizing mouse anti-TGF-β1 monoclonal antibody (Clone 9016) and sheep anti-rat IgG magnetic bead-conjugated antibody (Cat. No.110-35) were purchased from R&D Systems (Minneapolis, MN, USA) and Invitrogen (Carlsbad, CA, USA), respectively. Recombinant VEGF 165 and PI-PLC were purchased from Santa Cruz Biotechnology (Santa Cruz, CA, USA) and Sigma–Aldrich (St. Louis, MO, USA), respectively. An R58 monoclonal antibody that recognizes neo-epitopes formed via the PLK-dependent proteolytic activation of latent TGF-β1 was produced and characterized as previously reported [10].

2.2. Animal experiments

One hundred microliters of saline with or without recombinant VEGF 165 was injected intravenously via the tail veins of three 10-week-old C57BL/6 male mice (Japan SLC Inc., Shizuoka, Japan) daily at doses of 10 or 20 ng/g body weight for 10 days. The mice were euthanized, and the livers were harvested for biochemical and immunohistochemical analyses. All animal experiments were performed in compliance with the protocols approved by the RIKEN Institutional Animal Use and Care Administrative Advisory Committee.

2.3. Staining of liver tissue sections

Liver tissues were fixed in 4% paraformaldehyde (PFA) and embedded in paraffin, and tissue sections (6-μm thick) were prepared using a Leica sliding microtome (Leica Microsystems, Nussloch, Germany). The liver tissue sections were deparaffinized, rehydrated and incubated for 5 min with a drop of Proteinase K (Dako Envision) in 2 ml of 0.05 M Tris–HCl buffer (pH 7.5) at room temperature. Thereafter, endogenous peroxidase was blocked by incubation with 3% hydrogen peroxide in methanol at room temperature for 10 min. The liver tissue sections were stained with Myer's hematoxylin solution and 1% Eosin Y solution (Muto Pure Chemicals, Tokyo, Japan). For CD31 staining, liver sections were incubated at 4 °C overnight with rat anti-CD31 monoclonal antibody (5 μg/ml) and thereafter with the biotinylated rabbit anti-rat IgG antibody (1:200) included in the Vectastain Elite ABC kit for 30 min at room temperature. A 3,3′-diaminobenzidine (DAB) peroxidase substrate kit (Vector Laboratories, Inc., Burlingame, CA, USA) was used for its chromogenic substrate, which develops as a brown precipitate, to visualize immunolabeling. For α-SMA staining, liver sections were incubated at 4 °C overnight with mouse anti-α-SMA monoclonal antibody (1:100) and thereafter with DAKO Envision's polymer of antibodies labeled with peroxidase for 1 h at room temperature. The DAB peroxidase substrate kit was used for its chromogenic substrate. Sirius red, which results in the red staining of all fibrillary collagen, was used to evaluate fibrosis. The liver sections were stained with 0.05% Fast-green FCF (ChemBlink, Inc., CAS 2353-45-9) and 0.05% Direct red 80 (Polysciences, Inc., CAS 2610-10-18) in saturated picric acid (Muto Pure Chemicals) for 90 min at room temperature. Positive area analyses were performed using the WinROOF image analysis software from 3 randomly selected fields among 3 mice for a total of 9 samples per group.

2.4. Measurement of hepatic hydroxyproline content

The hepatic hydroxyproline content was measured as described by Reddy et al. [15]. Briefly, approximately 40 mg of frozen liver tissue was hydrolyzed in 2 N NaOH for 10 min at 65 °C, followed by incubation at 120 °C for 20 min. The same amount of 6 N HCl was added and incubated at 120 °C for 20 min. Activated charcoal solution (10 mg/ml in 4 N KOH) and 2.2 M acetic acid–0.48 M citric acid buffer (pH 6.5) were added to adjust the pH to 7–8. After centrifugation, 100 mM chloramine T solution was added to the supernatant and incubated at room temperature for 25 min. After the addition of 1 M Ehrlich's solution (*p*-dimethylaminobenzaldehyde), samples were incubated at 65 °C for 20 min. Absorbance was measured at 560 nm. The hydroxyproline content is expressed in μg/mg of sample protein.

2.5. Isolation of HSCs and LSECs

Primary HSCs were isolated from the livers of male C57BL/6 mice by collagenase/pronase digestion and the Nycodenz gradient method as described previously [9]; the cells were then cultured in Dulbecco's modified Eagle's medium (DMEM) containing 10% fetal bovine serum (FBS). Primary LSECs were isolated using a combination of rat anti-CD146 and sheep anti-rat IgG antibodies conjugated with magnetic beads from a fraction separated using the Nycodenz gradient method after the collagenase digestion of the livers of male C57BL/6 mice, according to the method described by Kitazume et al. [16]. The cells were then cultured in a DMEM/nutrient mixture F-12 (F12) containing 10% FBS.

2.6. Preparation of the LSEC conditioned medium (CM)

Briefly, 1×10^5 LSECs were seeded onto 6-well plates and precultured for 24 h with DMEM/F12 containing 10% FBS medium to grow the cells to confluency, followed by overnight starvation with DMEM/F12 containing 2% FBS at 37 °C. After the cells were rinsed with phosphate buffered saline (PBS), the medium was changed to 2 ml of DMEM/F12 containing 2% FBS and further cultured for 24 h to create LSEC CM.

2.7. Immunofluorescent staining

HSCs were fixed with 4% PFA for 10 min and incubated with 0.1% Triton X-100 in PBS for 20 min at room temperature. After blocking with 3% BSA in PBS for 40 min at room temperature, cells were incubated with FITC-conjugated anti-mouse α-SMA monoclonal antibody (1:200) for 2 h at room temperature. After being washed with PBS, the cells were mounted with Vectashield DAPI mounting medium (Vector Laboratories, Inc., Burlingame, CA, USA) and observed under a Zeiss LSM 700 laser scanning confocal microscope. The intensities of α-SMA and R58 LAP-DPs were calculated in each panel with ZEN software for quantitative fluorescence analyses.

2.8. Determination of the TGF-β concentration in CM

TGF-β was measured using a bioassay (luciferase assay in CCL64 cells) for active TGF-β and an enzyme-linked immunosorbent assay (ELISA) for total TGF-β. CCL64 cells, from the mink lung epithelial cell line, stably expressing $(CAGA)_9$-MLP-luciferase, which contains nine copies of an Smad binding CAGA box element upstream of a minimal adenovirus major late promoter [17], were plated at 2×10^4 cells/well in a 96-well plate with DMEM containing 10% FBS. On the next day, the medium was replaced with CM harvested from HSCs. After 6 h, the cells were extracted with a lysis buffer, and luciferase activity was measured using a Luciferase Assay System (Promega, Madison, WI, USA) according to the manufacturer's instructions. The amount of active TGF-β was calculated from a standard curve made with recombinant TGF-β1. The total TGF-β1 levels present in the LSEC CM before and after incubating with HSCs were determined using a TGF-β1 Emax immune Assay System ELISA kit (Promega, Madison, WI, USA) according to the manufacturer's instructions. Samples were acidified using 1 N HCl to a pH of 3.0 for 15–20 min, followed by neutralization with 1 N NaOH before they were subjected to ELISA.

2.9. Real-time RT-PCR

Total RNA isolation and real-time RT-PCR were performed as described previously [18]. Briefly, total RNA was extracted using the RNeasy micro kit (Qiagen, Valencia, CA) according to the manufacturer's protocols. RNA (0.5 μg) was reverse transcribed to

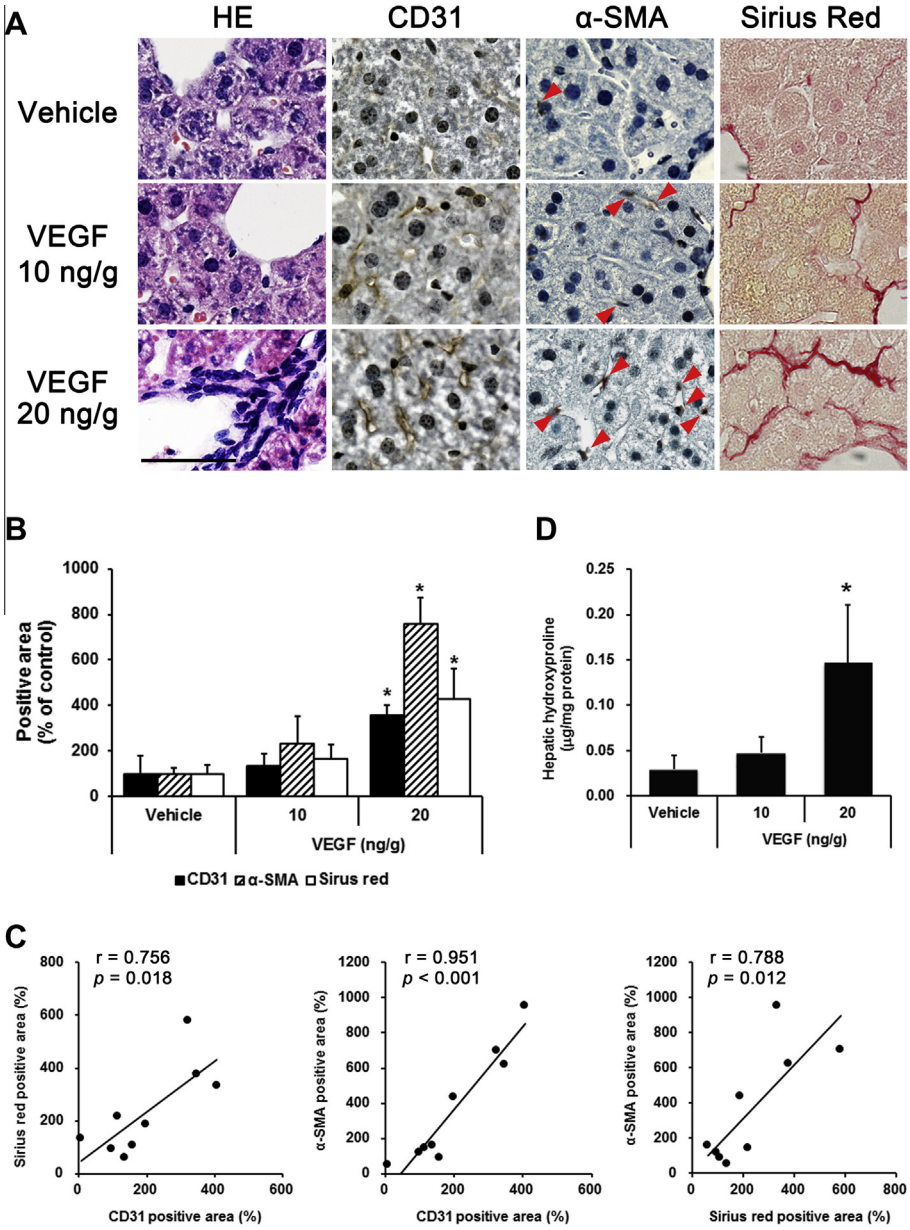

Fig. 1. VEGF simultaneously induced angiogenesis and fibrogenesis in the liver. Saline (100 μl/mouse/day) with or without recombinant VEGF at the indicated doses was injected into the tail vein of three 10-week-old C57BL/6 mice for 10 days. Their livers were removed after the animals were euthanized. (A) Liver tissue sections were prepared and stained with HE, antibodies for CD31 and α-SMA, and Sirius red, as described in the Section 2. Scale bar is 50 μm. Red arrow heads represent α-SMA positive cells. (B) CD31, α-SMA and Sirius red-positive areas (%) were quantitated and plotted as the means ± SD in the bar graphs ($n = 3$). (C) The correlation between CD31 and Sirius red-positive area (left panel), CD31 and α-SMA-positive area (middle panel), and Sirius red- and α-SMA-positive area (right panel). (D) The liver HDP levels were measured as described in the Section 2. *$p < 0.05$ compared with vehicle-treated mice.

cDNA using the PrimeScript® RT Master Mix (Takara Bio Inc., Shiga, Japan). mRNA expression levels were determined using real-time PCR. Real-time PCR was performed with the Thermal Cycler Dice® Real Time System using the SsoAdvanced™ SYBR® Green Supermix (Bio-Rad Laboratories, Hercules, CA) and normalized to 18S rRNA expression. The primer sequences used were as follows: mouse TGF-β1 forward: 5′-GCA ACA ATT CCT GGC GTT ACC-3′, reverse: 5′-CCC TGT ATT CCG TCT CCT TGG T-3′; mouse PLK forward: 5′-GAC CAG AGT ACC GGA AGA AG-3′, reverse: 5′-ACC TAT CTC CGA AAG CGC AC-3′; mouse uPAR forward: 5′-GCC GCT ATC CTA CAG AGC AC-3′, reverse: 5′-GCT ATG GAA ACC TGC TGT GCC-3′; and 18S rRNA forward: 5′-GTA ACC CGT TGA ACC CCA TT-3′, reverse: 5′-CCA TCC AAT CGG TAG TAG CG-3′.

2.10. Statistics

Statistical analyses were performed using one-way analysis of variance, followed by the Dunnett's or Tukey's post hoc tests. A two-tailed Student's *t*-test was used to evaluate the differences between the two groups.

3. Results

3.1. Simultaneous induction of hepatic angiogenesis and fibrogenesis in mice after injection of VEGF

VEGF administration to mice dose-dependently increased the number of cellular infiltrations, endothelial cells (CD31 staining, 3.6-fold at 20 ng VEGF/g of BW), and active HSCs (α-SMA staining, red arrow heads, 7.6-fold at 20 ng VEGF/g of BW), which accompanied an increase in the Sirius red-positive area (4.3-fold at 20 ng VEGF/g of BW) (Fig. 1A and B). Significant correlations were observed among the positive areas of CD31, α-SMA, and Sirius red (Fig. 1C). The hepatic hydroxyproline levels also increased 5-fold at 20 ng VEGF/g of BW (Fig. 1D) and 10-fold at 30 ng VEGF/g of BW (data not shown).

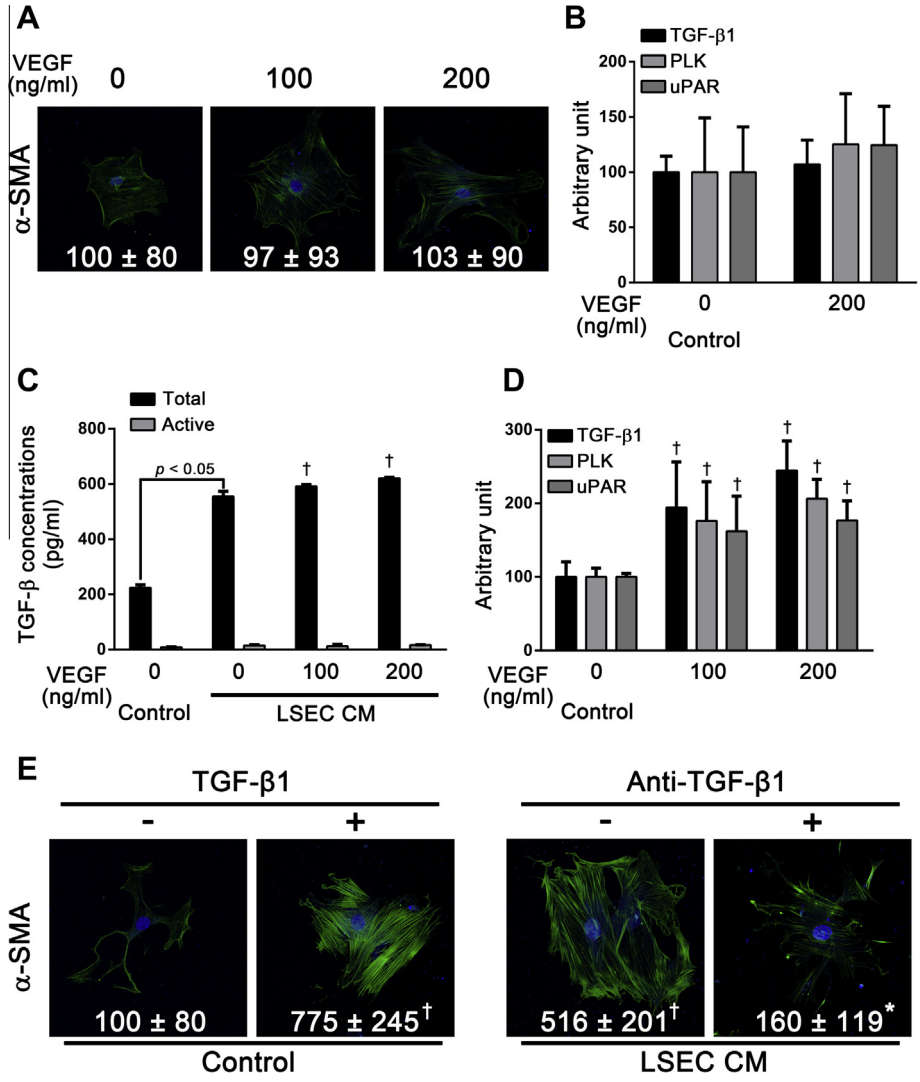

Fig. 2. LSEC CM enhanced HSC activation via TGF-β. Primary HSCs were incubated with 2% FBS DMEM in the presence or absence of the indicated concentrations of recombinant VEGF (A and B), TGF-β1 (100 pg/ml), and LSEC CM in the presence or absence of neutralizing anti-TGF-β1 (2.5 μg/ml) (E) for 5 days. Primary LSECs were incubated with 2% FBS DMEM/F12 in the presence or absence of the indicated concentrations of recombinant VEGF for 24 h (C and D). (A and E) Cells were fixed and stained with α-SMA as described in the Section 2. The relative fluorescence intensities (% of untreated control cells) are shown as the mean ± SD. (B and D) The mRNA expression levels of TGF-β1, PLK, and uPAR were measured using real-time RT-PCR as described in the Section 2. (C) Total/active TGF-β1 levels in the media were measured as described in the Section 2. †$p < 0.05$ compared with untreated control cells, *$p < 0.05$ compared with LSEC CM-treated control cells.

3.2. The enhancement of the activation of HSCs with VEGF-treated LSEC CM via TGF-β

We investigated the molecular mechanism through which VEGF induces hepatic fibrosis in mice using primary cell culture systems. As assessed by the lack of an increase in the α-SMA levels (a marker of activated HSCs), VEGF did not directly activate isolated primary HSCs after 5 days of treatment at 100 and 200 ng/ml, concentrations that are nearly equivalent to the blood concentration of VEGF in in vivo experiments (Fig. 2A). VEGF also did not affect the mRNA expressions of TGF-β1, PLK, and uPAR (Fig. 2B). VEGF enhanced latent TGF-β1 concentration (1.1-fold at 200 ng/ml VEGF) in LSEC CM (Fig. 2C) and mRNA expressions of TGF-β1 (2.4-fold at 200 ng/ml VEGF), PLK (2.1-fold at 200 ng/ml VEGF), and uPAR (1.8-fold at 200 ng/ml VEGF) in LSECs (Fig. 2D). HSCs were activated via incubation with recombinant TGF-β1 (100 pg/ml) and LSEC CM, the latter of which was blocked by incubation with neutralizing antibodies against TGF-β1 (Fig. 2E).

3.3. Latent TGF-β secreted from LSECs is activated by PLK on the surface of HSCs

Given the ELISA and bioassay results, we found that primary LSECs secreted only 2.5% of TGF-β in the active form during 24 h incubation (Fig. 2C), and that the active TGF-β concentrations in LSEC CM were slightly higher than those in the control medium (DMEM containing 2% FBS) (Fig. 2C). To investigate whether latent TGF-β present in LSEC CM was activated by PLK as we previously showed [9], we cultured primary HSCs with LSEC CM with or without PI-PLC, which cleaves the glycophosphatidylinositol anchor, re-

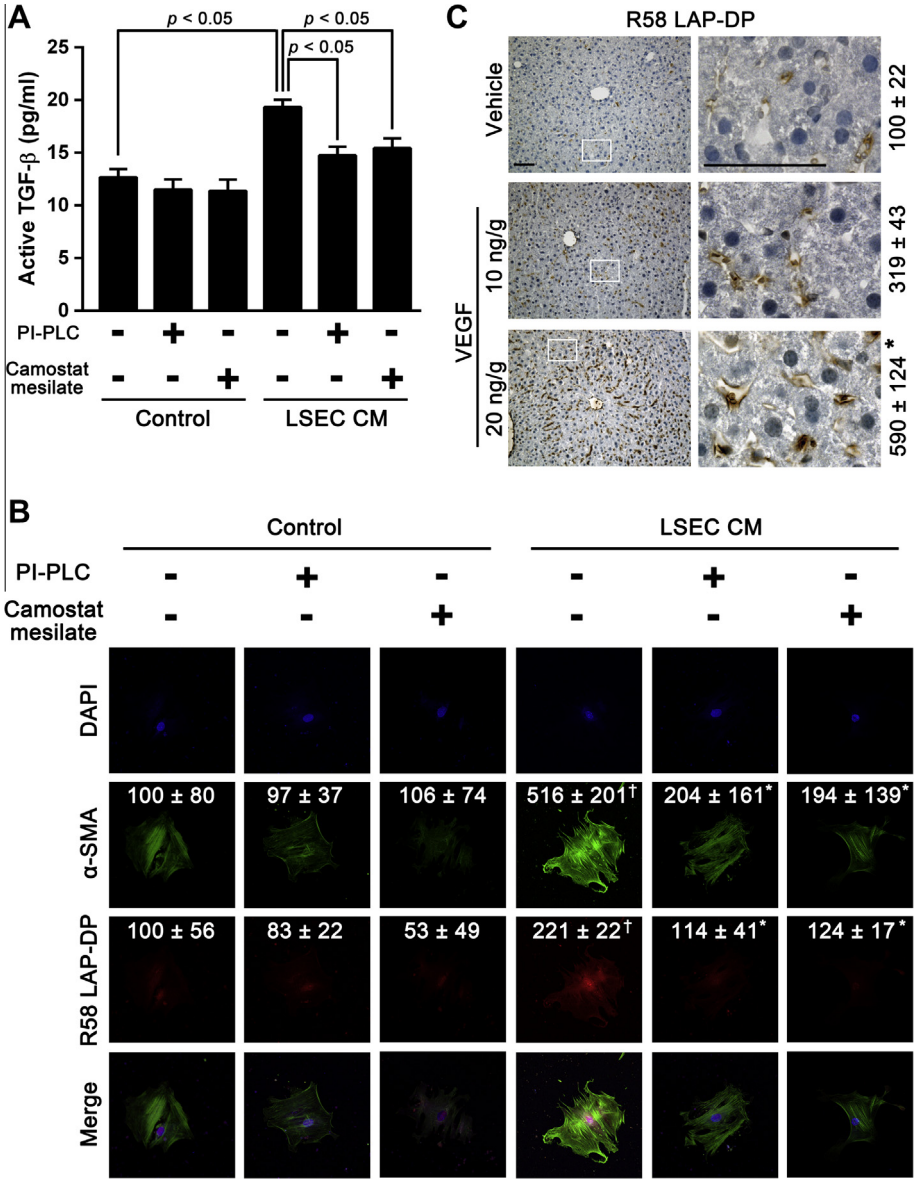

Fig. 3. Latent TGF-β derived from LSECs was activated on the surface of hepatic stellate cells through PLK in in vitro and in vivo. Primary HSCs were incubated with 2% FBS DMEM or LSEC CM in the presence or absence of PI-PLC (0.5 U/mL) or camostat mesilate (500 μM) for 5 days. (A) Active TGF-β1 levels in the media were measured using the luciferase assay in $(CAGA)_9$-Luc CCL64 cells. Data are shown as the means ± SD. (B) Cells were fixed and stained with α-SMA and R58 LAP-DPs as described in the Section 2. The relative fluorescence intensities (% of untreated control cells) are shown as the means ± SD. (C) The liver sections harvested from the VEGF-injected mice were stained with anti-R58 LAP-DPs antibody, as described in the Section 2. The right panels show higher magnifications of the corresponding white squares in the left panels. Scale bars, 100 μm. Positive areas (%) were quantitated and shown as the means ± SD ($n = 3$). $^{\dagger}p < 0.05$ compared with untreated control cells, $^{*}p < 0.05$ compared with LSEC CM-treated control cells.

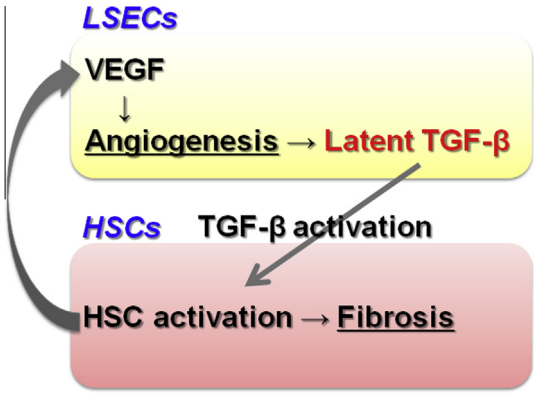

Fig. 4. The scheme of the molecular mechanism through which angiogenesis promotes fibrosis in the liver. Increased neovessels provided with latent TGF-β, which PLK activates on the surface of HSCs and stimulates the activation of HSCs. Therefore, angiogenesis might accelerate liver fibrosis.

leases uPAR and its associated with PLK from the cell surface, or with or without camostat mesilate, a serine protease inhibitor. Both these treatments resulted in a reduction in the concentration of active TGF-β in the LSEC CM (Fig. 3A). LSEC CM failed to activate the HSCs that had been incubated with either PI-PLC or camostat mesilate (Fig. 3B). The R58 LAP-DP levels, a footprint of PLK-dependent TGF-β activation [9], were reduced via either PI-PLC or camostat mesilate. VEGF did not affect R58 LAP-DPs expression (Relative fluorescent intensity: Control 100 ± 56; VEGF 100 ng/ml 112 ± 30; VEGF 200 ng/ml 99 ± 48). To confirm whether PLK-dependent activation might be increased along with neovessel formation in vivo, the liver sections harvested from the VEGF-administered mice were stained with anti-R58 LAP-DPs antibody. As expected, the R58-positive area was increased with VEGF injection by 5.9-fold (Fig. 3C).

4. Discussion

In the present study, we addressed a role of ECs as a source of latent TGF-β, the precursor of the most fibrogenic cytokine TGF-β. We provided in vitro evidence that LSEC CM promotes the activation of quiescent HSCs via the provision of latent TGF-β and in vivo evidence that much more severe fibrosis was induced in the livers of mice that received VEGF (Fig. 4). These data suggest that HSC activation is promoted not only via changes in the extracellular matrix, inflammatory cytokines, and oxidative stress but also secondarily via pathological angiogenesis.

We documented that TGF-β, which is secreted from LSECs as a latent form and activated on the surface of mainly HSCs rather than LSECs (compare Figs. 3A and 2C), mediates enhancement in liver fibrosis, although the expressions of PLK and uPAR increased 2-fold in VEGF-treated LSECs (Fig. 2D). Several groups have reported that VEGF enhanced the expression of urokinase-type plasminogen activator and its receptor uPAR in both bovine microvascular endothelial cells and human umbilical vein endothelial cells [19], enabling them matrix degradation and cell invasion [20], and that bradykinin production via the PLK-dependent cleavage of high molecular weight kininogen promotes angiogenesis via the upregulation of basic fibroblast growth factor [21]. In our study, increased PLK in LSECs might interact with HSCs and promote TGF-β activation on the surface of HSCs. At the same time, increased uPAR and PLK in LSECs also might contribute to angiogenesis. We showed that VEGF increased the levels of hepatic CD31 by 3.6-fold and R58 LAP-DPs by 5.9-fold in mice and that VEGF enhanced latent TGF-β production and TGF-β1 mRNA expression in primary LSECs. These data also suggest that LSECs serve as the source of TGF-β for liver fibrosis.

Yoshiji et al. demonstrated that VEGF receptor expression increased in HSCs along with the development of fibrosis and that a neutralizing anti-VEGF receptor antibody attenuated both angiogenesis and fibrogenesis in the liver [22], using activated HSCs, whereas we used quiescent HSCs. The result in Fig. 1 suggests that VEGF promotes the growth of LSECs, which appears to serve as a source of latent TGF-β, thereby increasing the hepatic levels of TGF-β1, due to the increased number of LSECs in the early stages of liver fibrosis (Fig. 4). Eventually, HSCs were activated and began to express the VEGF receptor, respond to VEGF, and transition to a more activated state. However, we cannot rule out the involvement of other soluble factors, such as PDGF, which is also produced from LSECs and stimulates HSC activation [11,23].

Sorafenib, a multikinase inhibitor recently approved to treat unresectable hepatocellular carcinoma, was beneficial in a model of BDL-induced cirrhosis [24,25]. We have provided here evidence that angiogenesis accelerates liver fibrosis. The anti-fibrotic effect of sorafenib might be caused by its blocking of angiogenesis. Moreover, other anti-angiogenic treatments such as vatalanib [26] and bevacizumab [27], are now being evaluated in clinical cancer treatment trials. An implication of the current study is that anti-angiogenic agents such as vatalanib and bevacizumab might be beneficial for anti-fibrotic therapy in addition to sorafenib.

Acknowledgments

This work was supported in part by a Grant-in-Aid for Scientific Research from the Ministry of Education, Culture, Sports, Science and Technology (23390202 to S.K.), Grants for Collaborative Researchers from Industries (to K.S.), the Uehara Memorial Foundation, Japan (to S.K.), and the Research on the Innovative Development and the Practical Application of New Drugs for Hepatitis B (Principal investigator: Soichi Kojima; H24-B Drug Discovery-Hepatitis-General-003) provided by the Ministry of Health, Labor and Welfare of Japan.

References

[1] S.L. Friedman, Mechanisms of hepatic fibrogenesis, Gastroenterology 134 (2008) 1655–1669.
[2] R. Bataller, D.A. Brenner, Liver fibrosis, J. Clin. Invest. 115 (2005) 209–218.
[3] N.C. Henderson, T.D. Arnold, Y. Katamura, M.M. Giacomini, J.D. Rodriguez, J.H. McCarty, A. Pellicoro, E. Raschperger, C. Betsholtz, P.G. Ruminski, D.W. Griggs, M.J. Prinsen, J.J. Maher, J.P. Iredale, A. Lacy-Hulbert, R.H. Adams, D. Sheppard, Targeting of αv integrin identifies a core molecular pathway that regulates fibrosis in several organs, Nat. Med. 19 (2013) 1617–1624.
[4] S.L. Friedman, Hepatic stellate cells: protean, multifunctional, and enigmatic cells of the liver, Physiol. Rev. 88 (2008) 125–172.
[5] H. Tsukamoto, Cytokine regulation of hepatic stellate cells in liver fibrosis, Alcohol. Clin. Exp. Res. 23 (1999) 911–916.
[6] F.R. Weiner, M.A. Giambrone, M.J. Czaja, A. Shah, G. Annoni, S. Takahashi, M. Eghbali, M.A. Zern, Ito-cell gene expression and collagen regulation, Hepatology 11 (1990) 111–117.
[7] M. Matsuoka, N.T. Pham, H. Tsukamoto, Differential effects of interleukin-1α, tumor necrosis factor α, and transforming growth factor β1 on cell proliferation and collagen formation by cultured fat-storing cells, Liver 9 (1989) 71–78.
[8] S.B. Jakowlew, J.E. Mead, D. Danielpour, J. Wu, A.B. Roberts, N. Fausto, Transforming growth factor-β (TGF-β) isoforms in rat liver regeneration: messenger RNA expression and activation of latent TGF-β, Cell Regul. 2 (1991) 535–548.
[9] K. Akita, M. Okuno, M. Enya, S. Imai, H. Moriwaki, N. Kawada, Y. Suzuki, S. Kojima, Impaired liver regeneration in mice by lipopolysaccharide via TNF-α/kallikrein-mediated activation of latent TGF-β, Gastroenterology 123 (2002) 352–364.
[10] S. Kojima, Detection of hepatic fibrogenesis targeting proteolytic TGF-β activation reaction, Hepatology (2008) 917A.
[11] D. Thabut, V. Shah, Intrahepatic angiogenesis and sinusoidal remodeling in chronic liver disease: new targets for the treatment of portal hypertension?, J Hepatol. 53 (2010) 976–980.
[12] B.S. Ding, D.J. Nolan, J.M. Butler, D. James, A.O. Babazadeh, Z. Rosenwaks, V. Mittal, H. Kobayashi, K. Shido, D. Lyden, T.N. Sato, S.Y. Rabbany, S. Rafii,

Inductive angiocrine signals from sinusoidal endothelium are required for liver regeneration, Nature 468 (2010) 310–315.
[13] M. Fernandez, D. Semela, J. Bruix, I. Colle, M. Pinzani, J. Bosch, Angiogenesis in liver disease, J. Hepatol. 50 (2009) 604–620.
[14] H. Sahin, E. Borkham-Kamphorst, C. Kuppe, M.M. Zaldivar, C. Grouls, M. Al-samman, A. Nellen, P. Schmitz, D. Heinrichs, M.L. Berres, D. Doleschel, D. Scholten, R. Weiskirchen, M.J. Moeller, F. Kiessling, C. Trautwein, H.E. Wasmuth, Chemokine Cxcl9 attenuates liver fibrosis-associated angiogenesis in mice, Hepatology 55 (2012) 1610–1619.
[15] G.K. Reddy, C.S. Enwemeka, A simplified method for the analysis of hydroxyproline in biological tissues, Clin. Biochem. 29 (1996) 225–229.
[16] S. Kitazume, R. Imamaki, K. Ogawa, Y. Komi, S. Futakawa, S. Kojima, Y. Hashimoto, J.D. Marth, J.C. Paulson, N. Taniguchi, α2,6-sialic acid on platelet endothelial cell adhesion molecule (PECAM) regulates its homophilic interactions and downstream antiapoptotic signaling, J. Biol. Chem. 285 (2010) 6515–6521.
[17] P.K. Datta, H.L. Moses, STRAP and Smad7 synergize in the inhibition of transforming growth factor β signaling, Mol. Cell. Biol. 20 (2000) 3157–3167.
[18] K. Sakata, M. Hara, T. Terada, N. Watanabe, D. Takaya, S. Yaguchi, T. Matsumoto, T. Matsuura, M. Shirouzu, S. Yokoyama, T. Yamaguchi, K. Miyazawa, H. Aizaki, T. Suzuki, T. Wakita, M. Imoto, S. Kojima, HCV NS3 protease enhances liver fibrosis via binding to and activating TGF-β type I receptor, Sci. Rep. 3 (2013) 3243.
[19] S.J. Mandriota, G. Seghezzi, J.D. Vassalli, N. Ferrara, S. Wasi, R. Mazzieri, P. Mignatti, M.S. Pepper, Vascular endothelial growth factor increases urokinase receptor expression in vascular endothelial cells, J. Biol. Chem. 270 (1995) 9709–9716.
[20] J.M. Breuss, P. Uhrin, VEGF-initiated angiogenesis and the uPA/uPAR system, Cell Adh. Migr. 6 (2012) 535–615.
[21] R.W. Colman, Regulation of angiogenesis by the kallikrein–kinin system, Curr. Pharm. Des. 12 (2006) 2599–2607.
[22] H. Yoshiji, S. Kuriyama, J. Yoshii, Y. Ikenaka, R. Noguchi, D.J. Hicklin, Y. Wu, K. Yanase, T. Namisaki, M. Yamazaki, H. Tsujinoue, H. Imazu, T. Masaki, H. Fukui, Vascular endothelial growth factor and receptor interaction is a prerequisite for murine hepatic fibrogenesis, Gut 52 (2003) 1347–1354.
[23] J.S. Lee, D. Semela, J. Iredale, V.H. Shah, Sinusoidal remodeling and angiogenesis: a new function for the liver-specific pericyte?, Hepatology 45 (2007) 817–825
[24] D. Thabut, C. Routray, G. Lomberk, U. Shergill, K. Glaser, R. Huebert, L. Patel, T. Masyuk, B. Blechacz, A. Vercnocke, E. Ritman, R. Ehman, R. Urrutia, V. Shah, Complementary vascular and matrix regulatory pathways underlie the beneficial mechanism of action of sorafenib in liver fibrosis, Hepatology 54 (2011) 573–585.
[25] M. Mejias, E. Garcia-Pras, C. Tiani, R. Miquel, J. Bosch, M. Fernandez, Beneficial effects of sorafenib on splanchnic, intrahepatic, and portocollateral circulations in portal hypertensive and cirrhotic rats, Hepatology 49 (2009) 1245–1256.
[26] J.M. Wood, G. Bold, E. Buchdunger, R. Cozens, S. Ferrari, J. Frei, F. Hofmann, J. Mestan, H. Mett, T. O'Reilly, E. Persohn, J. Rosel, C. Schnell, D. Stover, A. Theuer, H. Towbin, F. Wenger, K. Woods-Cook, A. Menrad, G. Siemeister, M. Schirner, K.H. Thierauch, M.R. Schneider, J. Drevs, G. Martiny-Baron, F. Totzke, PTK787/ZK 222584, a novel and potent inhibitor of vascular endothelial growth factor receptor tyrosine kinases, impairs vascular endothelial growth factor-induced responses and tumor growth after oral administration, Cancer Res. 60 (2000) 2178–2189.
[27] N. Ferrara, K.J. Hillan, H.P. Gerber, W. Novotny, Discovery and development of bevacizumab, an anti-VEGF antibody for treating cancer, Nat. Rev. Drug. Discovery 3 (2004) 391–400.